Experimental and numerical investigation on the laminar flame speed of CH4/O2 mixtures diluted with CO2 and H2O

Antoine Mazas, Deanna A. Lacoste, Thierry Schuller

Proceedings of ASME Turbo Expo 2010: Power for Land, Sea and Air
GT2010
June 14-18, 2010, Glasgow, UK

GT2010-22512

EXPERIMENTAL AND NUMERICAL INVESTIGATION ON THE LAMINAR FLAME SPEED OF CH_4/O_2 MIXTURES DILUTED WITH CO_2 AND H_2O

A. N. Mazas*
Air Liquide, Centre de Recherche Claude-Delorme
Les Loges-en-Josas
F-78354 Jouy-en-Josas Cedex, France
Email: antoine.mazas@airliquide.com

D. A. Lacoste and T. Schuller†
Laboratoire EM2C, CNRS and Ecole Centrale Paris
Grande Voie des Vignes
F-92295 Chatenay-Malabry Cedex, France
Email: thierry.schuller@em2c.ecp.fr

ABSTRACT

The effects of CO_2 and H_2O addition on premixed oxy-fuel combustion are investigated with experiments and numerical simulations on the laminar flame speed of $CH_4/O_2/CO_2/H_2O_{(v)}$ and $CH_4/O_2/N_2/H_2O_{(v)}$ mixtures, at atmospheric pressure and for a reactants inlet temperature T_u = 373 K. Experiments are conducted with steady laminar conical premixed flames over a range of operating conditions representative of oxy-fuel combustion with flue gas recirculation. The relative O_2-to-CO_2 and O_2-to-N_2 ratios, respectively defined as $O_2/(O_2+CO_2)$ (mol.) and $O_2/(O_2+N_2)$ (mol.), are varied from 0.21 to 1.0. The equivalence ratio of the mixtures ranges from 0.5 to 1.5, and the steam molar fraction in the reactive mixture is varied from 0 to 0.45. Laminar flame speeds are measured with the flame area method using a Schlieren apparatus. Experiments are completed by simulations with the PREMIX code using the detailed kinetic mechanism GRI-mech. 3.0. Numerical predictions are found in good agreement with experimental data for all cases explored. It is also shown that the laminar flame speed of $CH_4/O_2/N_2$ mixtures diluted with steam $H_2O_{(v)}$ features a quasi-linear decrease when increasing the diluent molar fraction, even at high dilution rates. Effects of N_2 replacement by CO_2 in wet reactive mixtures are then investigated. A similar quasi-linear decrease of the flame speed is observed for $CH_4/O_2/CO_2$ H_2O-diluted flames. For a similar flame speed in dry conditions, results show a larger reduction of the burning velocity for $CH_4/O_2/N_2/H_2O$ mixtures than for $CH_4/O_2/CO_2/H_2O$ mixtures, when the steam molar fraction is increased. Finally, it is observed that the laminar flame speed of weakly (CO_2, H_2O)-diluted CH_4/O_2 mixtures is underestimated by the GRI-mech 3.0 predictions.

NOMENCLATURE

$\mathcal{A}_f$ Flame area (m^2)
$\dot{m}$ Mass flow rate ($kg.s^{-1}$)
p Pressure (Pa)
s_u^o Laminar flame speed ($m.s^{-1}$)
s_T Turbulent burning velocity ($m.s^{-1}$)
T Temperature (K)
T_{ad} Adiabatic flame temperature (K)
X_i Molar fraction of species i
ρ density ($kg.m^{-3}$)
ϕ Equivalence ratio
Ω_i O_2 molar dilution ratio with respect to N_2 ($i = N$) or CO_2 ($i = C$)
RFG Recycled Flue Gas

INTRODUCTION

Oxy-fuel combustion technology has been identified as a promising approach for power generation with CO_2 capture and storage [1]. In this process, the fuel is burned in pure oxygen diluted with a large amount of recycled flue gas (RFG) in order to maintain exhaust temperatures compatible with materials thermal resistance. Carbon dioxide and water vapor are the main

*Address all correspondence to this author.
†Address all correspondence to this author.

components of the flue gas generated by oxy-combustion processes, thereby reducing significantly the cost of CO_2 separation. The presence of CO_2 and $H_2O_{(v)}$ in the reactive mixture in place of N_2 in traditional air-fuel combustion is likely to affect the combustion properties through thermal, chemical and radiative mechanisms. Additional research is thus required to characterize combustion in O_2/RFG environments [1]. Although many studies on oxy-fuel combustion are dedicated to solid fuels, especially coal (see e.g. the review proposed by Buhre *et al.* [2]), it is worthwhile investigating the effects of RFG dilution on gaseous fuels, which are also widely used in gas turbines for power generation.

Some effects of CO_2 addition and of $H_2O_{(v)}$ addition on flame characteristics have been *separately* examined in the last decades. A brief overview is given here on the main results obtained regarding CO_2-diluted and H_2O-diluted flames properties.

The effects of CO_2 addition on premixed flame structure have been examined for $CH_4/O_2/N_2/CO_2$ and $H_2/O_2/N_2/CO_2$ mixtures [3, 4]. Species concentrations were measured in a jet-stirred reactor for a wide range of equivalence ratios and temperatures, at p = 1 atm and 10 atm. It was observed that CO_2 inhibits the oxidation of H_2 and CH_4, reacting with H radicals in the reaction CO_2 + H = CO + OH (R1). This chain-carrying reaction competes for H atoms consumption with the chain-branching reactions H + O_2 = OH + H and H + HO_2 = OH + OH. The chemical effect of CO_2 in oxy-fuel combustion of methane was also discussed for high CO_2 concentrations. It was found that CO_2 dilution is likely to yield increased CO concentrations in the near-burner region due to the reaction (R1), having possible consequences for burner corrosion and slagging [5].

Ignition and extinction characteristics of CO_2-diluted reactive mixtures have also been examined. Homogeneous ignition was investigated with OH concentrations LIF-measurements in a catalytic channel-flow reactor for lean $CH_4/O_2/N_2/CO_2$ mixtures, at pressures p = 4 - 16 bar [6]. Extinction limits were measured as a function of stretch for CH_4/CO_2 (resp. CH_4/N_2) and O_2/CO_2 (resp. CH_4/N_2) counterflow non-premixed flames up to 7 bar [7]. While conventional C-shapes extinction behaviors were observed for $CH_4/O_2/N_2$ mixtures, the extinction limits of $CH_4/O_2/CO_2$ are broadened at low stretch rates at 5 and 7 bar. This phenomenon was attributed to radiation reabsorption due to the presence of CO_2 in fresh gases. The effects of radiative emission and absorption on the propagation and the extinction of premixed flames have also been studied numerically [8, 9] and experimentally [10]. Results show a significant contribution of non-grey radiation on flammability limits and burning velocities when increasing the pressure and the amount of CO_2 in the unburned gases.

The influence on soot formation of carbon dioxide addition in diffusion flames was studied experimentally [11–13] and numerically [14, 15]. The addition of CO_2 led to a significant decrease of soot volume fraction. It was shown that CO_2 dilution thermally and chemically limits the formation of soot precursors due to the decrease of H radicals consummed in the reaction CO_2 + H = CO + OH.

The effects of CO_2 addition on the burning velocity have been explored to discuss the validity domain of detailed kinetic mechanisms. However, existing studies are limited to highly diluted oxy-fuel mixtures or to air-fuel mixtures in which small CO_2 quantities are added. The chemical effect of CO_2 replacement of N_2 in air on the burning velocity of CH_4 and H_2 flames was numerically investigated [16]. Laminar flame speeds of CH_4/(Ar, N_2, CO_2)-air mixtures were measured for a wide range of equivalence ratios, pressure and flame temperatures [17]. Propagation speeds of flat flames were also measured with the heat flux method for different fuels (H_2, CH_4, C_2H_6, C_3H_8) in O_2/CO_2 environments with high CO_2 molar fractions [18–22]. In those studies, the O_2-to-CO_2 molar ratio, defined as $O_2/(O_2+CO_2)$ (mol.), ranges typically between 0.12 and 0.35. Laminar burning velocities were also measured for H_2/air/He/CO_2 mixtures with a constant volume spherical bomb [23].

The effects of CO_2 dilution on turbulent premixed flames were investigated for CH_4/air mixtures, at elevated pressure [24–26]. For small CO_2 concentrations – corresponding to CO_2 molar fractions X_{CO_2} ranging from 0 to 0.05, no difference was observed in the turbulent flame structure for a given pressure [26]. In experiments conducted with preheated mixtures (573 K) with a CO_2-to-air molar ratio $CO_2/(CO_2$+air) (mol.) varying between 0 and 0.10, the addition of CO_2 was found to affect the ratio of the turbulent burning velocity S_T normalized with the laminar burning velocity s_u^o, to increase the mean volume of the flame region and to modify the turbulent flame structure [24]. An increase of the bending of S_T/s_u^o versus u'/s_u^o plots was also observed when N_2 was replaced with CO_2 [25].

A few prior studies have also examined some effects of steam addition on premixed and non-premixed flames properties. Steam dilution is however less commonly investigated because of significant experimental difficulties to accurately control the quantity of steam injected in the reactive mixtures. Steam addition has soon been identified as a successful way to lower pollutant emissions – especially NO_x emissions – in gas turbines operating both in premixed and non-premixed modes [27–33]. This is particularly attractive when considering the continuous developments in Humid Air Turbine (HAT) cycles. In the most recent studies, it was shown that steam addition in various combustible mixtures (natural gas, *n*-heptane, *iso*-octane) led to substantial reductions of NO_x emissions, due to the decrease of the flame temperature and of O-atom concentration [34, 35]. Operating at constant adiabatic flame temperature, water vapor dilution was found to reduce NO_x levels by more than a factor of two compared to nitrogen dilution [36]. It was also observed that steam

addition had a very limited impact on CO emissions for a fixed flame temperature [34, 35].

The influence of steam as a fire inhibitor in premixed methane-air flames has been investigated. Regarding the thermal suppression effect, water vapor was found to be more effective than other gaseous thermal agents (N_2 and CF_4) or some chemical agents (CF_3Br) but less effective than the same mass of water mist [37]. These studies are however mainly based on numerical simulations and corresponding experiments were limited yet to small concentrations of added water vapor (steam mass fraction $Y_{H_2O} < 0.02$) [37, 38].

The effects of water vapor addition on flame extinction and ignition have also been examined recently. Critical conditions of ignition and extinction for hydrogen and methane flames were measured and calculated as a function of the water mass fraction in the oxidizer [40, 41]. It was observed that steam addition favors extinction and narrows regimes of ignition for premixed and non-premixed flames. Chemical effects of steam addition in hydrogen-air and methane-air flames were mainly attributed to the chaperon efficiency of water in three body reactions. This was also investigated experimentally with a jet-stirred reactor, at pressures p_u = 1 and 10 bar [42]. The oxidation of hydrogen and methane with 10% (mol.) of water vapor was studied with ignition delays and species concentrations measurements that were compared with computed species profiles. Kinetic modelling analysis shows that the chemical effect of steam results from H_2O high third body efficiency in the reaction H + O_2 + M = HO_2 + M.

Finally, the effects of steam addition on the laminar burning velocity were examined in different experiments. Burning velocities of hydrogen-air-steam and hydrogen-oxygen-steam mixtures were measured with laminar conical flames, for a wide range of steam molar fractions [43, 44]. Results show a significant decrease of the flame speed when water vapor is added. Laminar burning velocities of methane-air-steam were also measured using spherically expanding flames in a constant volume vessel filled with CH_4/air/$H_2O_{(v)}$ mixtures [45]. Measurements were carried out for stoichiometric mixtures over a wide range of initial pressures and for a constant unburned gas temperature T_u = 473 K, with a water vapor molar fraction varying from 0 to 0.20. Burning velocities were deduced from direct photographs of the early stage of the flame propagation. Results at atmospheric pressure show a quasi-linear decrease of the burning velocity when the water vapor molar fraction is increased, but data were not reported yet for non-stoichiometric or oxygen-enriched mixtures.

It is worthwhile noting that, regarding the effects of steam and carbon dioxide addition in flames, experimental and numerical results have been almost exclusively obtained for weakly diluted air-fuel mixtures or for highly diluted oxy-fuel mixtures, i.e. for mixtures whose flame temperatures are typically lower than 2250 K. In this work, experiments and numerical simulations are conducted to examine the simultaneous effects of CO_2 and H_2O addition on the laminar burning velocity of oxygen-enriched methane flames, at atmospheric pressure. Carbon dioxide and water vapor concentrations are chosen in order to explore a large domain of flame temperatures, from about 2000 to 3000 K.

EXPERIMENTAL SET-UP

Experiments are conducted on an oxycombustion-dedicated setup, including heated gas feeding lines, a steam production apparatus and an axisymetric burner on which steady conical laminar premixed flames are stabilized.

An overview of the experimental setup is shown in Fig. 1. Methane (CH_4), oxygen (O_2), nitrogen (N_2) and carbon dioxide (CO_2) gases (purity $>$ 99.99 %) are supplied from an external network of tanks. The flow rates of CH_4, O_2 and CO_2 (respectively N_2) are regulated with mass flow controllers (Bronkhorst F-Series), previously calibrated with the related gas. The accuracy of the mass flow controllers is $\pm$ 2 % of the set operating condition. Water vapor is produced with a custom-built apparatus derived from Cellkraft P-50 humidifier. Oxygen and carbon dioxide (respectively oxygen and nitrogen) are premixed before being introduced as a carrier gas in the humidifier. Steam production is based on the humidification of the carrier gas by transfer of water vapor through specific membranes (Nafion® membranes, DuPont). The carrier gas flows in membrane tubes, which are immersed in demineralized liquid water heated with electrical resistances. At the tubes exit, the carrier gas is saturated with steam. The dew point temperature T_{dew} of the humidified mixture is then measured with a humidity sensor (Vaisala Humicap Series HMT 330). A closed loop control of humidity based on the measured dew point temperature T_{dew} is used to regulate the temperature T_{lw} of the liquid water in which the membrane tubes are immersed. This temperature T_{lw} is varied to control the dew point of O_2/CO_2/H_2O (resp. O_2/N_2/H_2O) mixtures obtained at the humidifier outlet. The steam molar fraction $X^*_{H_2O}$ in the humidified carrier gas can then be inferred from the steam partial pressure p_{H_2O}, equal to the saturation vapor pressure at the dew-point temperature $p_{sat}(T_{dew})$, and from the humidifier inner pressure p_h, measured with a high temperature pressure transducer (Huba Control) placed at the humidifier outlet:

$$X^*_{H_2O} = \frac{p_{H_2O}}{p_h} = \frac{p_{sat}(T_{dew})}{p_h} \quad (1)$$

Experimental steam mass flow rates were measured and compared with theoretical predictions obtained with Eq. 1, as shown in Tab. 1. Experimental results are in good agreement with theoretical predictions, within 1% accuracy. It can be concluded from

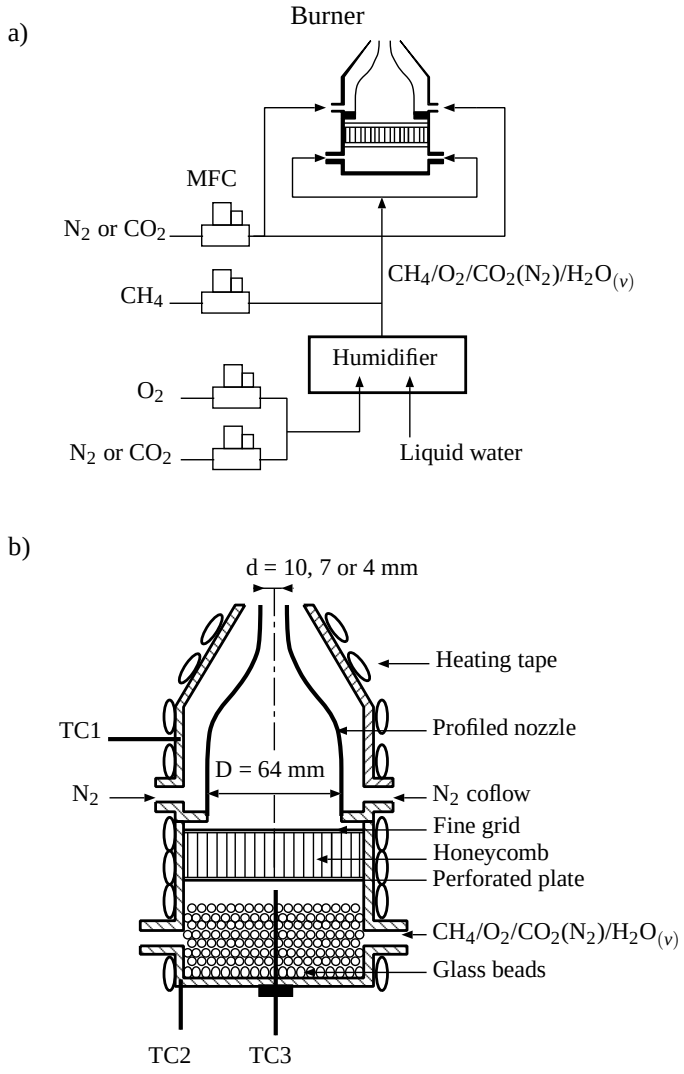

Figure 1: Schematic of the experimental set-up. a) Overview of the global set-up. b) Detailed view of the burner.

the humidifier linear operation and from the excellent repeatability of these tests that the steam concentration is remarkably stable and accurately controlled.

The $O_2/CO_2/H_2O$ (resp. $O_2/N_2/H_2O$) mixtures coming from the humidifier and methane flow are premixed before being introduced in an axisymmetric burner. A detailed view of the burner is shown in Fig. 1. Gases are injected in the lower part of the burner, which is filled with glass beads (1 to 5 mm diameter) to further reduce possible mixture non-homogeneities. The reactive mixture then flows successively through a perforated plate, a honeycomb structure and a refined metallic grid to obtain a laminar flow entering the inlet of a profiled converging nozzle. The burner can be equipped with three different converging nozzles of outlet diameter d = 10, 7 or 4 mm, with respective contraction

Humidifier performances: operating conditions [a]

$\dot{m}_{cg}$ (g/h)	p_h (mbar)	T_{dew} (K)	X_{H_2O}	$\dot{m}_{H_2O}$ (g/h)	
				Exp.	*Theor.*
776.3	1010	320	0.10	56.2	56.1
2329.0	1010	320	0.10	166.8	168.4
776.3	1217	350	0.42	254.6	253.0
2329.0	1692	350	0.42	474.2	475.6

[a] Carrier gas mass flow rate, humidifier pressure, dew point temperature, steam molar fraction, experimental and theoretical steam mass flow rates.

Table 1: Comparison of experimental and theoretical steam mass flow rates for various operating conditions.

ratios $\sigma = (D/d)^2$ = 41, 86 and 256. The converging nozzle is used to reduce the boundary layer thickness by accelerating the flow and to obtain a top hat velocity profile at the burner outlet. A small co-flow of nitrogen surrounding the inner main nozzle is used to prevent potential outer perturbations. The velocity profile at the burner outlet was characterized using a hot wire anemometry system (Dantec). It was checked that the velocity profile remains flat over 80% of the burner diameter and the RMS fluctuations were found to be less than 1.0 % of the mean velocity.

The temperature of all the components downstream the humidifier is controlled and set at the unburned gas temperature T_u to prevent water condensation. The burner temperature is regulated with an electrical heating tape (Vulcanic) and the temperature field homogeneity is simultaneously controlled with a J-type thermocouple TC1 inserted in the burner body and with a K-type thermocouple TC2 inserted in the bottom plate of the burner. A K-type thermocouple TC3 located immediately upstream the perforated plate is used to measure the mixture temperature T_u.

Schlieren images are obtained using a classical Z-arrangement with lenses (diameter 100 mm, focal length 1000 mm) and vertical knives (Ealing) to highlight horizontal density gradients. Pictures are recorded with a video CCD camera (768x576 square pixels, Pulnix), equipped with a variable speed shutter and a 100-300 mm lens (Cosina) to zoom in the flame region.

EXPERIMENTAL METHOD AND CALCULATIONS

The laminar burning velocity s_u^o is defined as the velocity at which a laminar, steady, plane, unstretched, adiabatic flame moves relative to the unburned premixed gas in a direction normal to the flame surface [46]. However, a flame fulfilling all the pre-cited requirements cannot be easily obtained experimentally and different experimental configurations can be employed, depending on the range of burning velocities explored and on the

nature of the reactive mixtures [47, 48]. In this study, it was chosen to work with steady conical $CH_4/O_2/CO_2(N_2)/H_2O_{(v)}$ flames stabilized on the burner outlet. The conical flame method is easy to implement, provides reliable results and has been successfully used in the past for oxy-fuel flame speeds measurements [44, 49]. Assuming the whole reactive mixture is burned, one can define an area-weighted average laminar flame speed $\bar{s_u}$ that can be calculated from the mass conservation equation $\dot{m} = \rho_u \bar{s_u} \mathcal{A}_f$, where $\dot{m}$ is the reactants mass flow rate, ρ_u is the unburned gas density and $\mathcal{A}_f$ is the flame area. Since the laminar burning velocity s_u^o is defined relative to the unburned gases, the most appropriated area is the upstream boundary of the preheat zone that can be determined with a Schlieren technique. When using a Schlieren imaging set-up, the light deflection due to optical index gradients is proportional to $|\nabla T|/T^2$, where T is the gas temperature [50]. As the maximum of light deflection occurs close to the upstream boundary of the preheat zone, the Schlieren technique is an efficient diagnostic to measure laminar burning velocities [51, 52]. The main disadvantages of conical flames are the heat losses at the burner rim and the effects of stretch and curvature that are known to affect the burning velocity [53]. Nevertheless, the high temperatures of oxygen-enriched flames induce limited heat losses compared to the total heat released by the flame and it is established that the hydrodynamic stretch is low for conical flames, since velocity gradients along the flame are small for conical flames stabilized in uniform flows [54]. The top-hat velocity profile at the burner outlet ensures that the flame speed is constant along the flame front, except near the flame tip and in the near-burner area [49]. Pictures of typical chemiluminescence and Schlieren images obtained in this work are shown in Fig. 2.

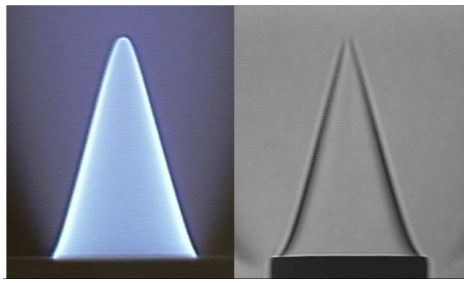

Figure 2: *Left: direct photograph of $CH_4/O_2/N_2$ flame, with $O_2/(O_2+N_2)$ (mol.) = 0.50 and ϕ = 1.50, at T_u = 373 K and atmospheric pressure. Right: corresponding Schlieren image. The Schlieren front is located close to the upstream boundary of the preheat zone.*

Experiments are completed by simulations of one-dimensional, freely propagating, unstretched, adiabatic, laminar, premixed flames using the PREMIX code of the CHEMKIN package [55]. This one-dimensional flame solver is employed with the detailed kinetic mechanism GRI mech. 3.0 [56].

RESULTS AND DISCUSSION

As it is discussed in the introduction, this work aims at providing new experimental data on the laminar flame speed of $CH_4/O_2/N_2/H_2O$ and $CH_4/O_2/CO_2/H_2O$ mixtures, with flame temperatures ranging from 2000 to 3000 K. The parameters examined in this work are: (a) the oxygen-enrichment ratios in the oxidizer $\Omega_N = X_{O_2}/(X_{O_2} + X_{N_2})$ and $\Omega_C = X_{O_2}/(X_{O_2} + X_{CO_2})$ where X_k is the molar fraction of the species k; (b) the steam molar fraction X_{H_2O} in the whole reactive mixture; (c) the mixture equivalence ratio $\phi = (\dot{m}_{CH_4}/\dot{m}_{O_2})/(\dot{m}_{CH_4}/\dot{m}_{O_2})_s$ where $(\dot{m}_{CH_4}/\dot{m}_{O_2})_s$ is the fuel-to-oxygen mass ratio in stoichiometric conditions. All the experiments are carried out at a constant unburned gas temperature $T_u = 373$ K $\pm$ 1 K, except for the case of $CH_4/Air/H_2O_{(v)}$ mixtures where the gas inlet temperature is set to $T_u = 473$ K $\pm$ 2 K so that the results can be compared to existing experimental data [45].

Typical operating conditions explored in this work are shown for stoichiometric mixtures in Tab. 2. In a first set of experiments, the oxygen concentration in the oxidizer is progressively increased, with Ω_N varying from 0.21 (air) to 1.0 (pure oxygen). Corresponding flame temperatures vary from 2260 K to 3060 K and computed laminar flame speeds vary from 55 cm/s to 409 cm/s. For each value of Ω_N, the corresponding ratio Ω_C is chosen in order to keep the same burning velocity. The flame temperatures for corresponding Ω_N and Ω_C ratios are found to be close. This allows to delineate four flame temperature ranges: $T_{ad} \sim$ 2250 K, 2500 K, 2800 K and 3000 K, for which the burning velocities of $CH_4/O_2/N_2/H_2O$ and $CH_4/O_2/CO_2/H_2O$ mixtures are measured, in lean (ϕ <1), stoichiometric (ϕ = 1) and rich conditions (ϕ >1).

Ω_N	$T_{ad}(\Omega_N)$ (K)	s_u^o (cm/s)	Ω_C	$T_{ad}(\Omega_C)$ (K)
0.21	2261	55	–	–
0.30	2548	112	0.52	2620
0.50	2825	223	0.72	2845
1.00	3060	409	1.00	3060

Table 2: Computed adiabatic flame temperatures and burning velocities of stoichiometric $CH_4/O_2/N_2$ and $CH_4/O_2/CO_2$ mixtures, at T_u = 373 K and p_u = 1 atm.

The present experimental procedure for the determination of the flame speed in wet environments is first validated with available experimental data. Results are compared for a stoichiomet-

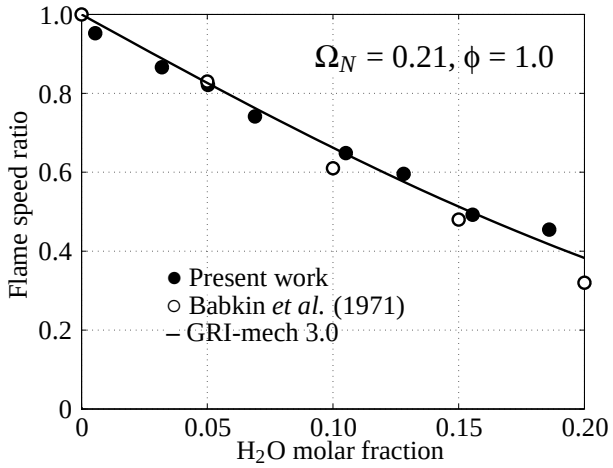

Figure 3: Experimental (symbols) and computed (lines) laminar flame speed ratios $\overline{s_u}(X_{H_2O})/\overline{s_u}(X_{H_2O}=0)$ of stoichiometric CH_4/Air/H_2O mixtures, at T_u = 473 K and atmospheric pressure.

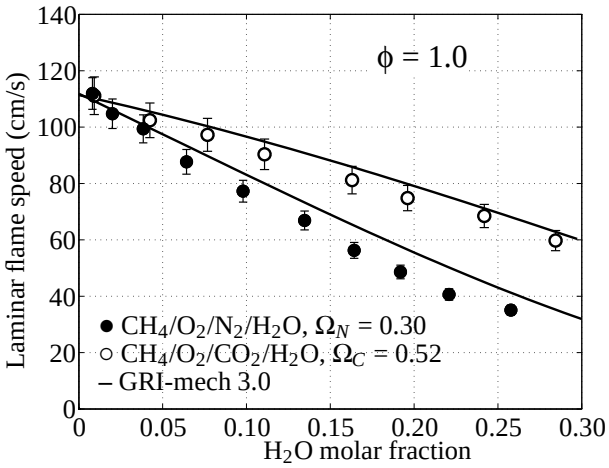

Figure 4: Experimental (symbols) and computed (lines) laminar flame speeds of $CH_4/O_2/N_2/H_2O$ and $CH_4/O_2/CO_2/H_2O$ mixtures, for $\Omega_N = X_{O_2}/(X_{O_2}+X_{N_2})$ = 0.30 and $\Omega_C = X_{O_2}/(X_{O_2}+X_{CO_2})$ = 0.52 respectively, ϕ = 1.0, at T_u = 373 K and atmospheric pressure.

ric methane/air flame at atmospheric pressure and preheated to $T_u = 473$ K with those obtained by Babkin *et al.* [45] with a spherical vessel. The evolution of the flame speed is plotted in Fig. 3 for H_2O molar fraction ranging from 0 to 0.20. It is found that the results obtained with different techniques match well and follow closely numerical predictions using the GRI-mech 3.0 kinetic mechanism. It is worth noting that the flame speed decreases almost linearly when the steam concentration is increased. Other tests, not shown here, were also conducted with dry methane/air mixtures and showed a good agreement with flame speed data obtained from the literature. This validates the methodology for the determination of the laminar burning velocity with a relative uncertainty of 5%.

All the remaining experiments are conducted at atmospheric pressure for preheated mixtures at $T_u = 373$ K and numerical simulations are performed with the GRI-mech 3.0 mechanism. The evolution of the flame speed is now examined in oxycombustion conditions for dry mixtures corresponding to an adiabatic flame temperature of about $T_{ad} \sim 2600$ K obtained with a nitrogen dilution ratio $\Omega_N = 0.30$ or a carbon dioxide dilution ratio $\Omega_C = 0.52$. Results are plotted in Figs. 4, 5 and 6 for stoichiometric ($\phi = 1$), lean ($\phi = 0.7$) and rich ($\phi = 1.4$) mixtures respectively, as a function of the steam molar fraction. It is worth noting that the flame speed measurements of dry stoichiometric mixtures diluted either with N_2 or CO_2 are equal as expected and reach about $\overline{s_u} = 1.1$ m.s^{-1} (Tab. 2). When increasing the steam molar fraction from 0 to 0.30, the flame speed features a larger decrease for a stoichiometric mixture diluted with nitrogen $\Omega_N = 0.30$ than with carbon dioxide $\Omega_C = 0.52$ (Fig. 4). Data are found in good agreement with numerical predictions in

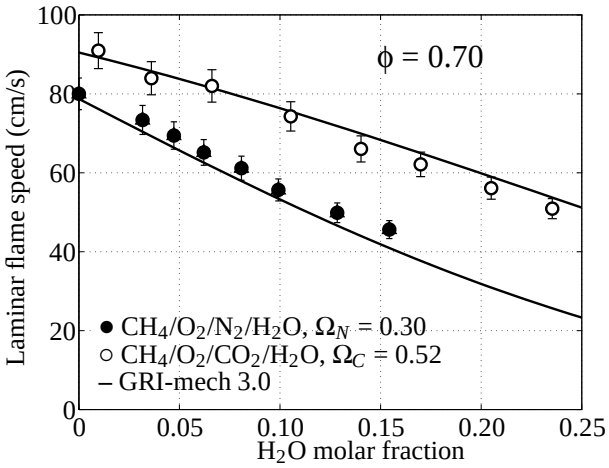

Figure 5: Experimental (symbols) and computed (lines) laminar flame speeds of $CH_4/O_2/N_2/H_2O$ and $CH_4/O_2/CO_2/H_2O$ mixtures, for $\Omega_N = X_{O_2}/(X_{O_2}+X_{N_2})$ = 0.30 and $\Omega_C = X_{O_2}/(X_{O_2}+X_{CO_2})$ = 0.52 respectively, ϕ = 0.70, at T_u = 373 K and atmospheric pressure.

both cases. These observations can also be made for lean and rich mixtures presented in Figs. 5 and 6 where experimental data closely match numerical simulations, even for high steam concentrations. The evolution of the flame speed of CO_2 diluted wet oxy-flames has however a slightly different concavity than that found for N_2 diluted wet oxy-flames.

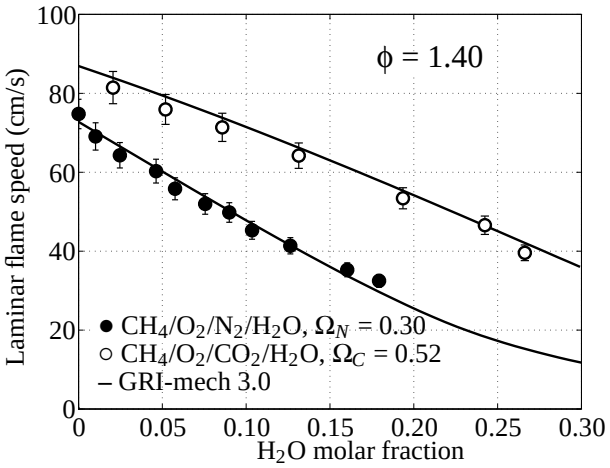

Figure 6: Experimental (symbols) and computed (lines) laminar flame speeds of $CH_4/O_2/N_2/H_2O$ and $CH_4/O_2/CO_2/H_2O$ mixtures, for $\Omega_N = X_{O_2}/(X_{O_2}+X_{N_2})$ = 0.30 and $\Omega_C = X_{O_2}/(X_{O_2}+X_{CO_2})$ = 0.52 respectively, ϕ = 1.40, at T_u = 373 K and atmospheric pressure.

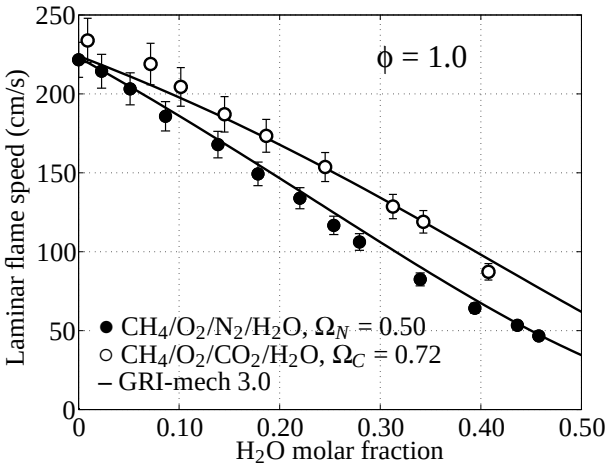

Figure 7: Experimental (symbols) and computed (lines) laminar flame speeds of $CH_4/O_2/N_2/H_2O$ and $CH_4/O_2/CO_2/H_2O$ mixtures, for $\Omega_N = X_{O_2}/(X_{O_2}+X_{N_2})$ = 0.50 and $\Omega_C = X_{O_2}/(X_{O_2}+X_{CO_2})$ = 0.72 respectively, ϕ = 1.0, at T_u = 373 K and atmospheric pressure.

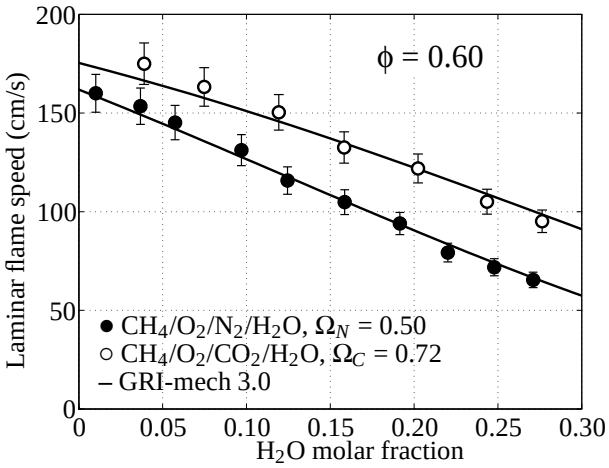

Figure 8: Experimental (symbols) and computed (lines) laminar flame speeds of $CH_4/O_2/N_2/H_2O$ and $CH_4/O_2/CO_2/H_2O$ mixtures, for $\Omega_N = X_{O_2}/(X_{O_2}+X_{N_2})$ = 0.50 and $\Omega_C = X_{O_2}/(X_{O_2}+X_{CO_2})$ = 0.72 respectively, ϕ = 0.60, at T_u = 373 K and atmospheric pressure.

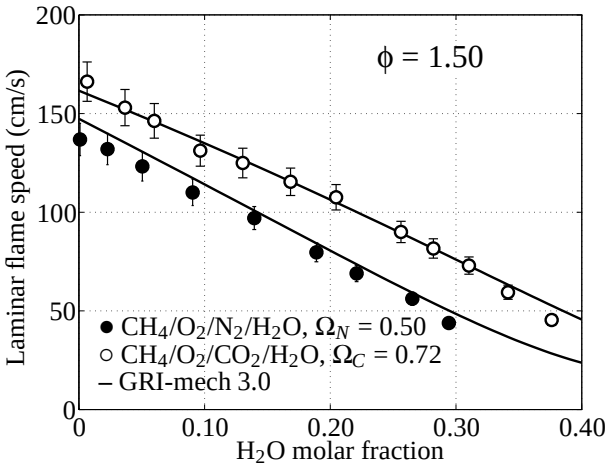

Figure 9: Experimental (symbols) and computed (lines) laminar flame speeds of $CH_4/O_2/N_2/H_2O$ and $CH_4/O_2/CO_2/H_2O$ mixtures, for $\Omega_N = X_{O_2}/(X_{O_2}+X_{N_2})$ = 0.50 and $\Omega_C = X_{O_2}/(X_{O_2}+X_{CO_2})$ = 0.72 respectively, ϕ = 1.50, at T_u = 373 K and atmospheric pressure.

Data are now reported for a higher concentration of oxygen in Figs. 7, 8 and 9. The same observations can be made for dry oxy-flames diluted with N_2 ($\Omega_N = 0.50$) and CO_2 ($\Omega_C = 0.72$). The flame speed of the dry stoichiometric mixture $\overline{s_u} = 2.2$ m.s^{-1} is now twice the value found in the previous case and corresponds to mixtures with a flame temperature of about $T_{ad} \sim 2800$ K. In stoichiometric conditions, the flame speed decrease is still more pronounced for N_2-diluted wet flames than for CO_2-diluted wet flames, but the difference is reduced because the oxygen ratio in the mixture has been increased. Numerical predictions still match closely the experimental data for stoichiometric ($\phi = 1$), lean ($\phi = 0.6$) or rich conditions ($\phi = 1.5$), up to high steam

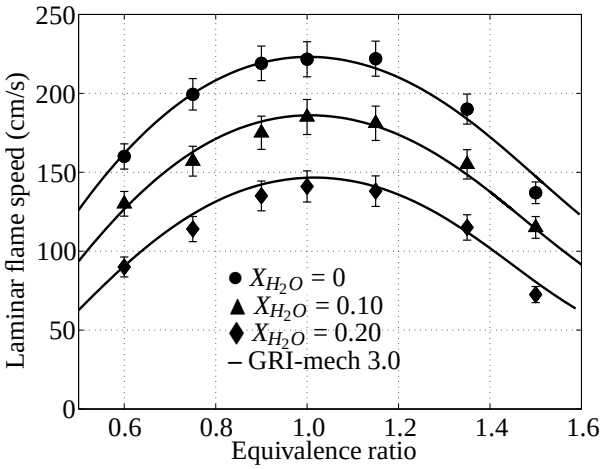

Figure 10: Experimental (symbols) and computed (lines) laminar flame speeds of $CH_4/O_2/N_2/H_2O$ mixtures as a function of the equivalence ratio, for $\Omega_N = X_{O_2}/(X_{O_2}+X_{N_2})$ = 0.50 and X_{H_2O} = 0, 0.10 and 0.20, at T_u = 373 K and atmospheric pressure.

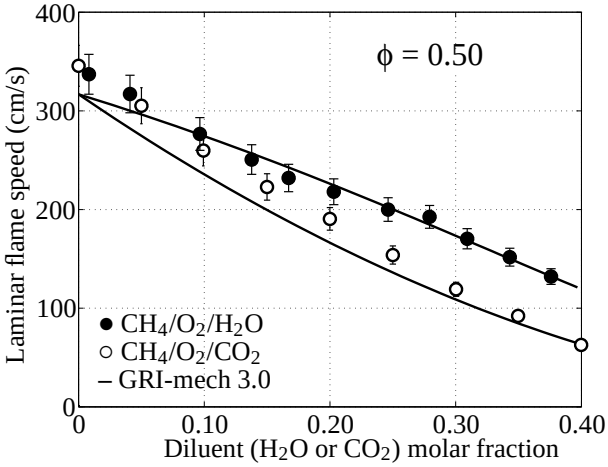

Figure 11: Experimental (symbols) and computed (lines) laminar flame speeds of $CH_4/O_2/H_2O$ and $CH_4/O_2/CO_2$ mixtures, for ϕ = 0.50, at T_u = 373 K and atmospheric pressure.

molar fractions $X_{H_2O} \sim 0.4$. The agreement between measurements and numerical predictions is observed to improve for results obtained at $T_{ad} = 2800$ K compared to those obtained at $T_{ad} = 2600$ K. This database is completed in Fig. 10 where the burning velocities of $CH_4/O_2/N_2/H_2O$ flames are plotted as a function of the equivalence ratio of the mixture. It is still found a good agreement between predictions and measurements of the flame speed for the three values of the steam molar fraction investigated $X_{H_2O} = 0$, 0.10 and 0.20 in the range $\phi = 0.60$ to 1.50.

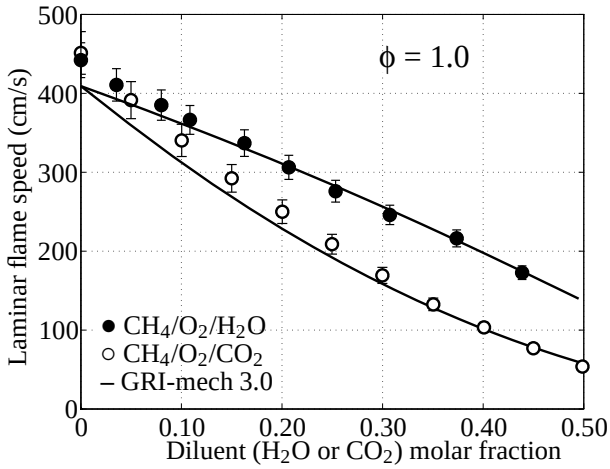

Figure 12: Experimental (symbols) and computed (lines) laminar flame speeds of $CH_4/O_2/H_2O$ and $CH_4/O_2/CO_2$ mixtures, for ϕ = 1.0, at T_u = 373 K and atmospheric pressure.

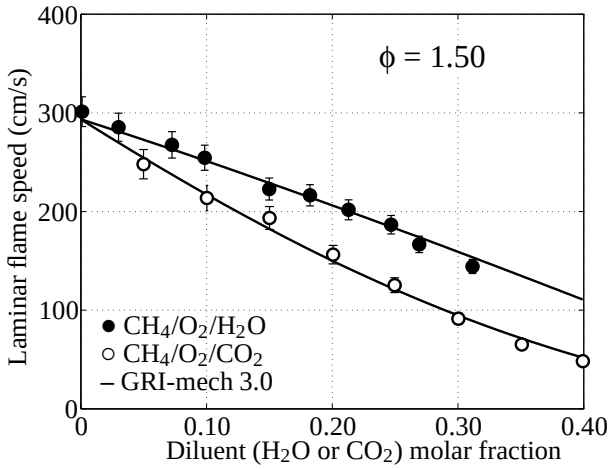

Figure 13: Experimental (symbols) and computed (lines) laminar flame speeds of $CH_4/O_2/H_2O$ and $CH_4/O_2/CO_2$ mixtures, for ϕ = 1.50, at T_u = 373 K and atmospheric pressure.

Effects of dilution by H_2O or CO_2 are now examined for oxy-fuel CH_4/O_2 flames. Results are plotted in Figs. 11, 12 and 13 for lean ($\phi = 0.50$), stoichiometric ($\phi = 1.0$) and rich ($\phi = 1.5$) mixtures respectively. When the laminar flame speed evolution is plotted as a function of the diluent molar fraction, a more pronounced decrease is observed for CO_2 dilution than for H_2O dilution. This is mainly due to the molar weight difference between H_2O (18 g/mol) and CO_2 (44 g/mol), although CO_2 features a slightly lower heat capacity than H_2O. For a same molar fraction of H_2O or CO_2 in the mixture, the flame temperature is lower for

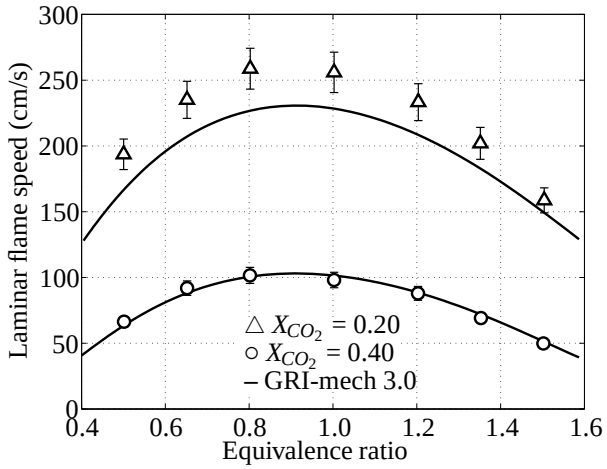

Figure 14: Experimental (symbols) and computed (lines) laminar flame speeds of $CH_4/O_2/CO_2$ mixtures as a function of the equivalence ratio for X_{CO_2} = 0.20 and 0.40, at T_u = 373 K and atmospheric pressure.

CO_2 addition than for H_2O addition. Consequently, the decrease rate of the flame speed is higher for CO_2-diluted flames than for H_2O-diluted flames. The general trend observed in these figures is correctly predicted by the simulations for all cases explored, but large differences are observed at low dilution rates for lean and stoichiometric flames. For dry CH_4/O_2 flames, simulations yield $s_u^o = 3.1$ m.s^{-1} and 4.0 m.s^{-1} for a lean ($\phi = 0.5$) and a stoichiometric mixture ($\phi = 1.0$). These predictions should be compared with the measurements yielding $s_u^o = 3.5$ m s^{-1} and 4.5 m s^{-1} in the same conditions. One can note that the GRI-mech 3.0 mechanism slightly underestimates the flame speed of CH_4/O_2 mixtures diluted with H_2O or CO_2, and that these differences reduce for higher dilution rates. The largest differences between experimental data and numerical predictions are observed for CO_2 dilution. These differences cancel for a rich mixture at $\phi = 1.5$. It is therefore interesting to examine the effects of equivalence ratio. The flame speed of methane/oxygen mixtures is plotted versus the equivalence ratio for two carbon dioxide molar fractions $X_{CO_2} = 0.20$ and 0.40 in Fig. 14. This figure clearly confirms that the predictions of the flame speed of CH_4/O_2 mixtures diluted with CO_2 are underestimated for equivalence ratios ranging from $\phi = 0.5$ to 1.50 for carbon dioxide molar fractions lower than $X_{CO_2} < 0.40$. The relative difference reaches about 10% for stoichiometric mixtures and reduces in lean and particularly in rich conditions. These differences between numerical predictions and measurements also cancel for highly CO_2-diluted oxy-fuel flames.

CONCLUSION

An experimental and numerical investigation on the laminar flame speed of CH_4/O_2 mixtures diluted with N_2, CO_2 and H_2O was conducted in this work. Laminar flame speeds were measured for a wide range of equivalence ratios ($0.50 < \phi < 1.50$), O_2-to-N_2 and O_2-to-CO_2 molar ratios ($0.21 < \Omega_N, \Omega_C < 1.0$) and steam molar fractions in the mixture ($0 < X_{H_2O} < 0.45$). It was observed that the laminar burning velocity of $CH_4/O_2/N_2/H_2O$ and $CH_4/O_2/CO_2/H_2O$ mixtures features a quasi-linear decrease when the steam molar fraction is increased. This decrease was found to be more pronounced for N_2-diluted than for CO_2-diluted wet mixtures. In these conditions, the flame speed is well predicted by the GRI-mech 3.0 mechanism. The effects of CO_2 and H_2O dilution were also investigated for oxy-fuel CH_4/O_2 flames. Experimental results show that GRI-mech 3.0 predictions underestimate the flame speeds at low H_2O ($X_{H_2O} < 0.10$) and CO_2 ($X_{CO_2} < 0.30$) dilution rates in lean and near-stoichiometric conditions, while differences reduce in rich conditions.

ACKNOWLEDGMENT

This work was supported by Air Liquide under the technical monitoring of Dr. B. Labégorre and Dr. R. Tsiava, and by the *Agence Nationale de la Recherche et de la Technologie* under a doctoral grant.

REFERENCES

[1] Wall, T. F., 2007. "Combustion processes for carbon capture". *Proceedings of the Combustion Institute,* ***31***, pp. 31–47.

[2] Buhre, B. J. P., Elliott, L. K., Sheng, C. D., Gupta, R. P., and Wall, T. F., 2005. "Oxy-fuel combustion technology for coal-fired power generation". *Progress in Energy and Combustion Science,* ***31***(4), pp. 283–307.

[3] Le Cong, T., and Dagaut, P., 2008. "Experimental and detailed kinetic modeling of the oxidation of methane and methane/syngas mixtures and effect of carbon dioxide addition". *Combustion Science and Technology,* ***180***, pp. 2046–2091.

[4] Le Cong, T., and Dagaut, P., 2009. "Oxidation of H_2/CO_2 mixtures and effect of hydrogen initial concentration on the combustion of CH_4 and CH_4/CO_2 mixtures: Experiments and modeling". *Proceedings of the Combustion Institute,* ***32***, pp. 427–435.

[5] Glarborg, P., and Bentzen, L. L. B., 2008. "Chemical effects of a high CO_2 concentration in oxy-fuel combustion of methane". *Energy & Fuels,* ***22***, pp. 291–296.

[6] Reinke, M., Mantzaras, J., Schaeren, R., Bombach, R., Inauen, A., and Schenker, S., 2005. "Homogeneous ignition of CH_4/air and H_2O and CO_2-diluted CH_4/O_2 mix-

tures over Pt; an experimental and numerical investigation at pressures up to 16 bar". *Proceedings of the Combustion Institute,* ***30***, pp. 2519–2527.

[7] Maruta, K., Abe, K., Hasegawa, S., Maruyama, S., and Sato, J., 2007. "Extinction characteristics of CH_4/CO_2 versus O_2/CO_2 counterflow non-premixed flames at elevated pressures up to 0.7 MPa". *Proceedings of the Combustion Institute,* ***31***, pp. 1223–1230.

[8] Ju, Y., Masuya, G., and Ronney, P. D., 1998. "Effects of radiative emission and absorption on the propagation and extinction of premixed gas flames". *Symposium (International) on Combustion,* ***27***(2), pp. 2619 – 2626.

[9] Ruan, J., Kobayashi, H., Niioka, T., and Ju, Y., 2001. "Combined effects of nongray radiation and pressure on premixed $CH_4/O_2/CO_2$ flames". *Combustion and Flame,* ***124***(1-2), pp. 225 – 230.

[10] Chen, Z., Qin, X., Xu, B., Ju, Y., and Liu, F., 2007. "Studies of radiation absorption on flame speed and flammability limit of CO_2 diluted methane flames at elevated pressures". *Proceedings of the Combustion Institute,* ***31***(2), pp. 2693–2700.

[11] Du, D. X., Axelbaum, R. L., and Law, C. K., 1995. "Soot Formation in Strained Diffusion Fames with Gaseous Additives". *Combustion and Flame,* ***102***(1-2), pp. 11–20.

[12] Zhang, C., Atreya, A., and Lee, K., 1992. "Sooting structure of methane counterflow diffusion flames with preheated reactants and dilution by products of combustion". *Twenty-Fourth Symposium (International) on Combustion,* ***24***(1), pp. 1049 – 1057.

[13] Oh, K. C., and Shin, H. D., 2006. "The effect of oxygen and carbon dioxide concentration on soot formation in non-premixed flames". *Fuel,* ***85***(5-6), pp. 615–624.

[14] Liu, F. S., Guo, H. S., Smallwood, G. J., and Gulder, O. L., 2001. "The chemical effects of carbon dioxide as an additive in an ethylene diffusion flame: Implications for soot and NO_x formation". *Combustion and Flame,* ***125***, pp. 778–787.

[15] Guo, H. S., and Smallwood, G. J., 2008. "A numerical study on the influence of CO_2 addition on soot formation in an ethylene/air diffusion flame". *Combustion Science and Technology,* ***180***(10-11), pp. 1695–1708.

[16] Liu, F. S., Guo, H. S., and Smallwood, G. J., 2003. "The chemical effect of CO_2 replacement of N_2 in air on the burning velocity of CH_4 and H_2 premixed flames". *Combustion and Flame,* ***133***(4), Jun, pp. 495–497.

[17] Zhu, D. L., Egolfopoulos, F. N., and Law, C. K., 1988. "Experimental and numerical determination of laminar flame speeds of Methane/(Ar, N_2, CO_2)-air mixtures as function of stoichiometry, pressure and flame temperature". *Twenty-Second Symposium (International) on Combustion,* ***22***, pp. 1537–1545.

[18] Konnov, A. A., and Dyakov, I., 2004. "Measurement of propagation speeds in adiabatic flat and cellular premixed flames of C_2H_6+O_2+CO_2". *Combustion and Flame,* ***136***(3), pp. 371–376.

[19] Konnov, A. A., and Dyakov, I. V., 2005. "Measurement of propagation speeds in adiabatic cellular premixed flames of CH_4+O_2+CO_2". *Experimental Thermal and Fluid Science,* ***29***(8), pp. 901–907.

[20] Konnov, A. A., and Dyakov, I. V., 2007. "Experimental study of adiabatic cellular premixed flames of Methane (Ethane, Propane) + Oxygen + Carbon Dioxyde mixtures". *Combustion Science and Technology,* ***179***, pp. 747–765.

[21] Coppens, F. H. V., and Konnov, A. A., 2008. "The effects of enrichment by H_2 on propagation speeds in adiabatic flat and cellular premixed flames of CH_4+O_2+CO_2". *Fuel,* ***87***(13-14), pp. 2866–2870.

[22] Kishore, V. R., Muchahary, R., Ray, A., and Ravi, M. R., 2009. "Adiabatic burning velocity of H_2-O_2 mixtures diluted with CO_2/N_2/Ar". *International Journal of Hydrogen Energy,* ***34***(19), pp. 8378–8388.

[23] Lamoureux, N., Djebaili-Chaumeix, N., and Paillard, C. E., 2003. "Laminar flame velocity determination for H_2-Air-He-CO_2 mixtures using the spherical bomb method". *Experimental Thermal and Fluid Science,* ***27***(4), pp. 385–393.

[24] Kobayashi, H., Hagiwara, H., Kaneko, H., and Ogami, Y., 2007. "Effects of CO_2 dilution on turbulent premixed flames at high pressure and high temperature". *Proceedings of the Combustion Institute,* ***31***, pp. 1451–1458.

[25] Shy, S. S., Chen, Y. C., Yang, C. H., Liu, C. C., and Huang, C. M., 2008. "Effects of H_2 or CO_2 addition, equivalence ratio, and turbulent straining on turbulent burning velocities for lean premixed methane combustion". *Combustion and Flame,* ***153***(4), pp. 510–524.

[26] Cohé, C., Chauveau, C., Gokalp, I., and Kurtulus, D. F., 2009. "CO_2 addition and pressure effects on laminar and turbulent lean premixed CH_4 air flames". *Proceedings of the Combustion Institute,* ***32***, pp. 1803–1810.

[27] Dryer, F., 1976. "Water addition to practical combustion systems – Concepts and applications". *Sixteenth Symposium (International) on Combustion,* ***16***, pp. 279 – 295.

[28] Miyauchi, T., Mori, Y., and Yamaguchi, T., 1981. "Effect of steam addition on NO formation". *Eighteenth Symposium (International) on Combustion,* ***18***, pp. 43 – 51.

[29] Touchton, G. L., 1985. "Influence of gas-turbine combustor design and operating parameters on effectiveness of NO_x suppression by injected steam or water". *Journal of Engineering for Gas Turbines and Power - Transactions of the ASME,* ***107***(3), pp. 706–713.

[30] Blevins, L. G., and Roby, R. J., 1995. "An experimental study of NO_x reduction in laminar diffusion flames by addition of high levels of steam". In ASME Paper 95-GT-327.

[31] Meyer, J.-L., and Grienche, G., 1997. "An experimental

study of steam injection in an aeroderivative gas turbine". In ASME Paper 97-GT-506.

[32] Correa, S. M., 1998. "Power generation and aeropropulsion gas turbines: from combustion science to combustion technology". *Twenty-Seventh Symposium (International) on Combustion*, pp. 1793–1813.

[33] Guo, H. S., Neill, W. S., and Smallwood, G. J., 2008. "A numerical study on the effect of water addition on NO formation in counterflow CH_4/air premixed flames". *Journal of Engineering for Gas Turbines and Power - Transactions of the ASME,* ***130***(5), pp. 054502–1–4.

[34] Bhargava, A., Colket, M., Sowa, W., Casleton, K., and Maloney, D., 2000. "An experimental and modeling study of humid air premixed flames". *Journal of Engineering for Gas Turbines and Power - Transactions of the ASME,* ***122***(3), pp. 405–411.

[35] de Jager, B., Kok, J. B. W., and Skevis, G., 2007. "The effects of water addition on pollutant formation from LPP gas turbine combustors". *Proceedings of the Combustion Institute,* ***31***, pp. 3123–3130.

[36] Landman, M. J., Derksen, M. A. F., and Kok, J. B. W., 2006. "Effect of combustion air dilution by water vapor or nitrogen on NO_x emission in a premixed turbulent natural gas flame: An experimental study". *Combustion Science and Technology,* ***178***(4), pp. 623–634.

[37] Fuss, S. P., Chen, E. F., Yang, W. H., Kee, R. J., Williams, B. A., and Fleming, J. W., 2002. "Inhibition of premixed methane/air flames by water mist". *Proceedings of the Combustion Institute,* ***29***, pp. 361–368.

[38] Thomas, G. O., 2002. "The quenching of laminar methane-air flames by water mists". *Combustion and Flame,* ***130***(1-2), pp. 147–160.

[39] Linteris, G. T., and Truett, L., 1996. "Inhibition of premixed methane-air flames by fluoromethanes". *Combustion and Flame,* ***105***(1-2), pp. 15 – 27.

[40] Seiser, R., and Seshadri, K., 2005. "The influence of water on extinction and ignition of hydrogen and methane flames". *Proceedings of the Combustion Institute,* ***30***(1), pp. 407 – 414.

[41] Yoo, C. S., Lee, S. D., and Chung, S. H., 2000. "Extinction of strained premixed flames of hydrogen/air/steam mixture: Local equilibrium temperature and local equivalence ratio". *Combustion Science and Technology,* ***155***, pp. 227–242.

[42] Le Cong, T., and Dagaut, P., 2008. "Effect of water vapor on the kinetics of combustion of hydrogen and natural gas: experimental and detailed modeling study". In ASME Paper GT2008-50272.

[43] Liu, D. D. S., and MacFarlane, R., 1983. "Laminar burning velocities of hydrogen-air and hydrogen-air-steam flames". *Combustion and Flame,* ***49***, pp. 59–71.

[44] Koroll, G., and Mulpuru, S., 1986. "The effect of dilution with steam on the burning velocity and structure of premixed hydrogen flames". *Twenty-First Symposium (International) on Combustion,* ***21***, pp. 1811 – 1819.

[45] Babkin, V. S., and V'yun, A. V., 1971. "Effect of water vapor on the normal burning velocity of a methane-air mixture at high pressures". *Fizika Goreniya i Vzryva,* ***7***(3), pp. 392–395.

[46] Law, C. K., 2006. *Combustion Physics*. Cambridge University Press.

[47] Andrews, G. E., and Bradley, D., 1972. "Determination of burning velocities - critical review". *Combustion and Flame,* ***18***, pp. 133–153.

[48] Rallis, C. J., and Garforth, A. M., 1980. "The determination of laminar burning velocity". *Progress in Energy and Combustion Science,* ***6***(4), pp. 303–329.

[49] Lewis, B., and Von Elbe, G., 1987. *Combustion, Flames and Explosions of Gases*, 3rd ed. Academic Press.

[50] Settles, G. S., 2001. *Schlieren and Shadowgraph Techniques*. Springer.

[51] Dunn-Rankin, D., and Weinberg, F., 1998. "Location of the Schlieren Image in Premixed Flames: Axially Symmetrical Refractive Index Fields". *Combustion and Flame,* ***113***, pp. 303–311.

[52] Durox, D., and Ducruix, S., 2000. "Concerning the location of the Schlieren limit in premixed flames". *Combustion and Flame,* ***120***, pp. 595–598.

[53] Law, C. K., 1988. "Dynamics of stretched flames". *Twenty-Second Symposium (International) on Combustion,* ***22***, pp. 1381–1402.

[54] Law, C. K., and Sung, C. J., 2000. "Structure, aerodynamics, and geometry of premixed flamelets". *Progress in Energy and Combustion Science,* ***26***, pp. 459–505.

[55] Kee, J., Grcar, K., Smooke, M., and Miller, J., 1985. PREMIX: A FORTRAN program for modelling steady laminar one-dimensional premixed flames. Technical report, Sandia National Laboratories.

[56] Smith, G. P., Golden, D. M., Frenklach, M., Moriarty, N. W., Eiteneer, B., Goldenberg, M., Bowman, C. T., Hanson, R. K., Song, S., Gardiner, Jr., W. C., Lissianski, V. V., and Qin, Z. http://www.me.berkeley.edu/gri_mech/.